The Astrophysical Journal, 688:1009–1020, 2008 December 1

A TRIO OF NEW LOCAL GROUP GALAXIES WITH EXTREME PROPERTIES

Alan W. McConnachie,[1] Avon Huxor,[2] Nicolas F. Martin,[3] Mike J. Irwin,[4] Scott C. Chapman,[4] Gregory Fahlman,[5] Annette M. N. Ferguson,[2] Rodrigo A. Ibata,[6] Geraint F. Lewis,[7] Harvey Richer,[8] and Nial R. Tanvir[9]

Received 2008 May 10; accepted 2008 June 24

ABSTRACT

We report on the discovery of three new dwarf galaxies in the Local Group. These galaxies are found in new CFHT/MegaPrime g, i imaging of the southwestern quadrant of M31, extending our extant survey area to include the majority of the southern hemisphere of M31's halo out to 150 kpc. All these galaxies have stellar populations which appear typical of dwarf spheroidal (dSph) systems. The first of these galaxies, Andromeda XVIII, is the most distant Local Group dwarf discovered in recent years, at ∼1.4 Mpc from the Milky Way (∼600 kpc from M31). The second galaxy, Andromeda XIX, a satellite of M31, is the most extended dwarf galaxy known in the Local Group, with a half-light radius of $r_h \sim 1.7$ kpc. This is approximately an order of magnitude larger than the typical half-light radius of many Milky Way dSphs, and reinforces the difference in scale sizes seen between the Milky Way and M31 dSphs (such that the M31 dwarfs are generally more extended than their Milky Way counterparts). The third galaxy, Andromeda XX, is one of the faintest galaxies so far discovered in the vicinity of M31, with an absolute magnitude of order $M_V \sim -6.3$. Andromeda XVIII, XIX, and XX highlight different aspects of, and raise important questions regarding, the formation and evolution of galaxies at the extreme faint end of the luminosity function. These findings indicate that we have not yet sampled the full parameter space occupied by dwarf galaxies, although this is an essential prerequisite for successfully and consistently linking these systems to the predicted cosmological dark matter substructure.

Subject headings: galaxies: dwarf — galaxies: individual (Andromeda XVIII, Andromeda XIX, Andromeda XX) — Local Group — surveys

Online material: color figures

1. INTRODUCTION

Edwin Hubble first coined the term "Local Group" in his 1936 book, *The Realm of the Nebulae*, to describe those galaxies that were isolated in the general field but were in the vicinity of the Galaxy. In recent years, the galaxies of the Local Group have been at the focus of intense and broad-ranging research, from providing laboratories for the investigation of dark matter properties (e.g., Gilmore et al. 2007 and references therein) to determinations of the star formation history of the universe (e.g., Skillman 2005 and references therein). Understanding individual galaxies in the Local Group offers important contributions to galaxy structure and evolution studies; understanding the properties of the population is central to galaxy formation in a cosmological context.

Hubble originally identified nine members of the Local Group: the Galaxy and the Large and Small Magellanic Clouds; M31, M32, and NGC 205; M33, NGC 6822, and IC 1613; along with three possible members, NGC 6946, IC 10, and IC 342. The distances of the latter three were highly uncertain due to heavy extinction; IC 10 has since been confirmed as a member (Sakai et al. 1999), although the other two lie outside the Local Group (NGC 6946: Sharina et al. 1997; IC 342: Krismer et al. 1995).

The discovery of new Local Group members continued at a relatively constant rate up to the start of 2004 (e.g., Ibata et al. 1994; Whiting et al. 1997, 1999; Armandroff et al. 1998, 1999; Karachentsev & Karachentseva 1999), at which point the discovery rate has increased sharply. This has mostly been due to large-area photometric CCD-based surveys of the Milky Way and M31 stellar halos: by searching for overdensities of resolved stars in certain regions of color-magnitude space, it is possible to identify very faint dwarf satellites which have previously eluded detection.

Around the Milky Way, this technique has so far lead to the discovery of 10 new satellites since 2005 (including possible diffuse star clusters; Willman et al. 2005, 2006; Belokurov et al. 2006, 2007; Zucker et al. 2006a, 2006b; Walsh et al. 2007; Sakamoto & Hasegawa 2006). All of these discoveries have been made using the Sloan Digitized Sky Survey (SDSS). In addition, two new isolated dwarf galaxies have been identified: Leo T, more than 400 kpc from the Milky Way (Irwin et al. 2007), was discovered in the SDSS, and a revised distance estimate for the previously known UGC 4879 has moved this galaxy from >10 Mpc to being placed on the periphery of the Local Group (a scant ∼1.1 Mpc from the Milky Way; Kopylov et al. 2008).

Around M31, nine new dwarf galaxy satellites have been discovered since 2004 (not including results presented herein). Two of these galaxies (Andromeda IX and X) were found in special SDSS scans of M31 (Zucker et al. 2004, 2007), and one (Andromeda XIV) was discovered serendipitously by Majewski et al. (2007) in Kitt Peak 4 m imaging of fields in the southeast

[1] Department of Physics and Astronomy, University of Victoria, Victoria, BC V8P 1A1, Canada; alan@uvic.ca.
[2] Institute for Astronomy, University of Edinburgh, Royal Observatory, Blackford Hill, Edinburgh EH9 3HJ, UK; huxor@roe.ac.uk, ferguson@roe.ac.uk.
[3] Max-Planck-Institut für Astronomie, Königstuhl 17, D-69117 Heidelberg, Germany; martin@mpia-hd.mpg.de.
[4] Institute of Astronomy, Madingley Road, Cambridge CB3 0HA, UK; mike@ast.cam.ac.uk, schapman@ast.cam.ac.uk.
[5] NRC Herzberg Institute of Astrophysics, 5071 West Saanich Road, Victoria, BC V9E 2E7, Canada; greg.fahlman@nrc-cnrc.gc.ca.
[6] Observatoire de Strasbourg, 11, rue de l'Universite, F-67000 Strasbourg, France; ibata@astro.u-strasbg.fr.
[7] Institute of Astronomy, School of Physics, A29, University of Sydney, NSW 2006, Australia; gfl@physics.usyd.edu.au.
[8] Department of Physics and Astronomy, University of British Columbia, Vancouver, BC V6T 1Z1, Canada; richer@phas.ubc.ca.
[9] Department of Physics and Astronomy, University of Leicester, Leicester LE1 7RH, UK; nrt3@star.le.ac.uk.

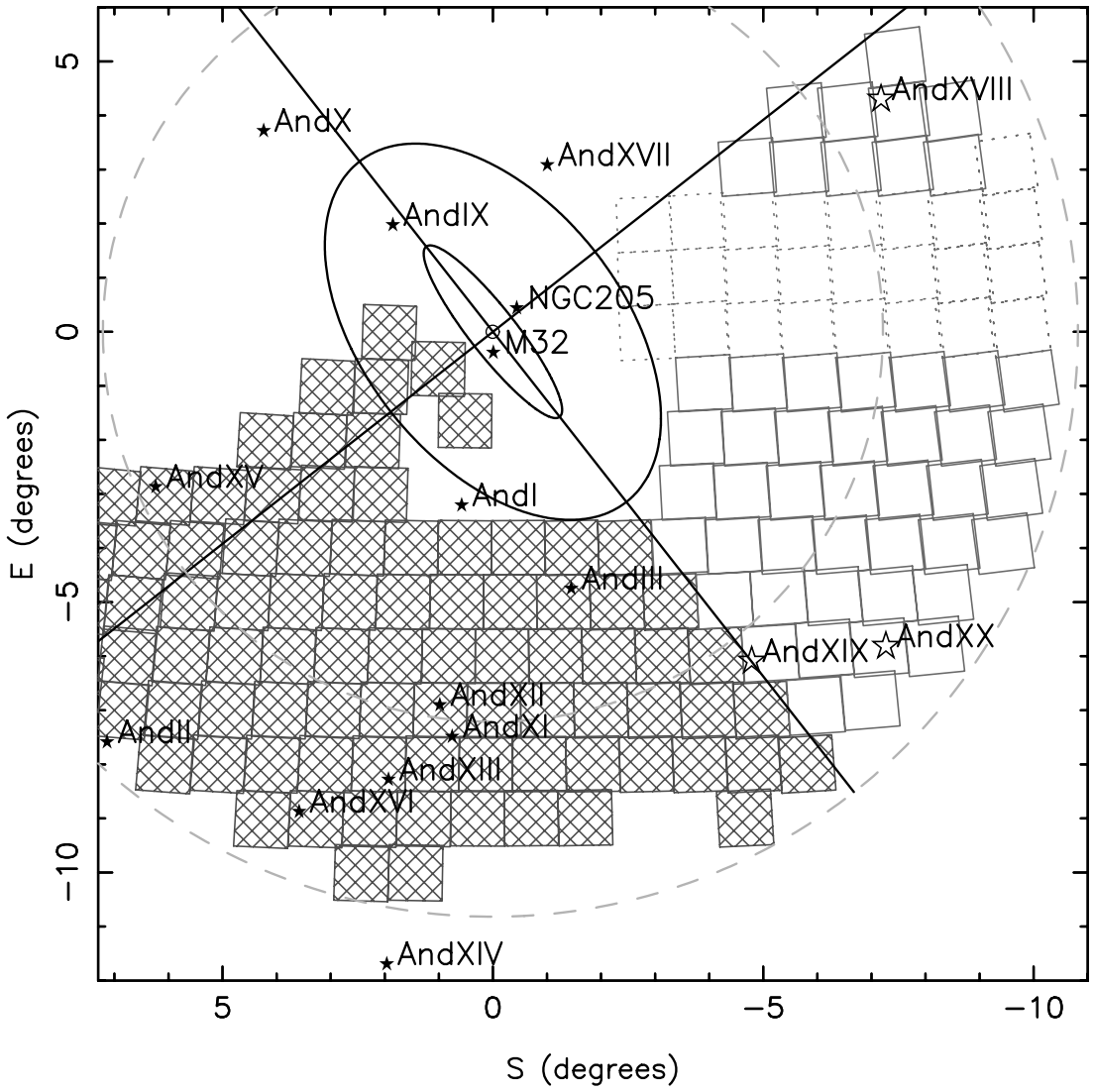

FIG. 1.—Tangent plane projection of the CFHT/MegaPrime survey area around M31. The inner ellipse represents a disk of inclination 77° and radius 2° (27 kpc), the approximate edge of the regular M31 disk. The outer ellipse shows a 55 kpc radius ellipse flattened to $c/a = 0.6$, the limit of the original INT/WFC survey (Ferguson et al. 2002). Major and minor axes of M31 are indicated. The inner and outer dashed circles show maximum projected distances of 100 and 150 kpc from the center of M31, respectively. Hatched fields show the location of our extant imaging of the southeast quadrant of M31 (Ibata et al. 2007). Light gray fields show the location of fields for our ongoing survey of the southwest quadrant of M31 (*solid lines denote observed fields; dotted lines denote fields still to be observed*). Black stars show the locations of various known M31 satellite galaxies, and open stars show the positions of the three new dwarf galaxies presented herein. [*See the electronic edition of the Journal for a color version of this figure.*]

halo of M31. The remaining new dwarf galaxies have been discovered as part of our ongoing photometric survey of this galaxy and its environs using the Isaac Newton Telescope Wide Field Camera (INT WFC) (Andromeda XVII; Irwin et al. 2008) and Canada-France-Hawaii Telescope (CFHT) MegaPrime (Andromeda XI, XII, and XIII: Martin et al. 2006; Andromeda XV and XVI: Ibata et al. 2007). Despite its name, Andromeda XVII is only the fifteenth dwarf spheroidal satellite of M31 to be discovered; Andromeda IV is a background galaxy (Ferguson et al. 2000), and Andromeda VIII was originally identified using planetary nebulae (Morrison et al. 2003) which were later shown to belong to M31 and not to a separate entity (Merrett et al. 2006). In addition, only 13 of these dwarfs are actually located in the constellation of Andromeda (Andromeda VI ≡ the Pegasus dSph; Andromeda VII ≡ the Cassiopeia dSph).

The unique, panoramic perspective of the resolved stellar populations of galaxies provided by Local Group members makes them ideal targets for observational programs aimed at understanding the detailed structure of galaxies, their formation processes, and their evolutionary pathways. Dwarf galaxies are of particular interest, given that they are thought to be the lowest mass, most dark matter dominated systems which contain baryons (e.g., Mateo 1998). They are therefore particularly sensitive probes of external processes, such as tides and ram pressure stripping (e.g., Mayer et al. 2006; McConnachie et al. 2007b; Peñarrubia et al. 2008b), and internal processes such as feedback from star formation (e.g., Dekel & Silk 1986; Dekel & Woo 2003). Furthermore, their potential as probes of dark matter (e.g., Gilmore et al. 2007; Strigari et al. 2007b) and their probable connection to cosmological substructures (e.g., Moore et al. 1999; Bullock et al. 2000; Kravtsov et al. 2004; Peñarrubia et al. 2008a) give them an importance to galaxy formation not at all in proportion to their luminosity.

Here we report on the discovery of three new dwarf galaxies in the Local Group, all of which have been found as part of our ongoing CFHT/MegaPrime photometric survey of M31. This

TABLE 1
PROPERTIES OF ANDROMEDA XVIII, XIX, AND XX

Parameter	Andromeda XVIII	Andromeda XIX	Andromeda XX
α (J2000.0)	00 02 14.5 ($\pm$10)	00 19 32.1 ($\pm$10)	00 07 30.7 ($\pm$15)
δ (J2000.0)	+45 05 20 ($\pm$10)	+35 02 37.1 ($\pm$10)	+35 07 56.4 ($\pm$15)
(l, b) (deg)	(113.9, $-$16.9)	(115.6, $-$27.4)	(112.9, $-$26.9)
$E(B-V)$	0.104	0.062	0.058
$I_{0,\,\mathrm{trgb}}$	21.62 $\pm$ 0.05	20.81 $\pm$ 0.05	$20.48^{+0.73}_{-0.20}$
$(m-M)_0$	25.66 $\pm$ 0.13	24.85 $\pm$ 0.13	$24.52^{+0.74}_{-0.24}$
Distance (kpc)	1355 $\pm$ 88	933 $\pm$ 61	802^{+297}_{-96}
r_{M31} (kpc)	$\sim$589	$\sim$187	$\sim$129
[Fe/H]	-1.8 ± 0.1	-1.9 ± 0.1	-1.5 ± 0.1
IQR	0.5	0.4	0.5
r_h (arcmin)	$0.92^{+0.05}_{-0.06}$	6.2 $\pm$ 0.1	$0.53^{+0.14}_{-0.04}$
r_h (pc)	363^{+31}_{-33}	1683 $\pm$ 113	124^{+56}_{-18}
P.A. (north to east) (deg)	0	(37^{+4}_{-8})	(80 $\pm$ 20)
$\epsilon = 1-b/a$	0	0.17 $\pm$ 0.02	0.3 $\pm$ 0.15
m_v	$\leq$16.0	15.6 $\pm$ 0.6	18.2 $\pm$ 0.8
M_V	≤ -9.7	-9.3 ± 0.6	$-6.3^{+1.0}_{-0.8}$
S_0	$\leq$25.6	29.3 $\pm$ 0.7	26.2 $\pm$ 0.8

NOTE.—Units of right ascension are hours, minutes, and seconds, and units of declination are degrees, arcminutes, and arcseconds. Values of ($\pm$10) and ($\pm$15) are in units of arcseconds.

new imaging extends our survey area from the southeastern quadrant discussed in Ibata et al. (2007) to the west, and currently includes an additional 49 deg^2 of M31's halo out to a maximum projected radius of 150 kpc. Section 2 summarizes the observations and data reduction procedures, and § 3 presents a preliminary analysis of the new dwarfs and quantifies their global properties. In § 4 we discuss our results in relation to some of the key questions which have been prompted with the discoveries of so many new low-luminosity galaxies in the Local Group. Section 5 summarizes our results.

2. OBSERVATIONS

Martin et al. (2006) and Ibata et al. (2007) presented the first results from our CFHT/MegaPrime survey of the southwest quadrant of M31, obtained in semesters S02B–06B. Since S06B, we have initiated an extension to this survey with the aim of obtaining complete coverage of the southern hemisphere of M31's halo out to a maximum projected radius of 150 kpc from the center of M31. Figure 1 shows the locations of these new fields relative to M31 in a tangent plane projection. Hatched fields represent those fields previously presented in Ibata et al. (2007). Light gray open fields represent the new survey area, where solid lines denote fields which were observed in S06B–07B, and dotted lines denote fields yet to be observed. Filled stars mark the positions of known M31 satellite galaxies, and open stars mark the positions of the three new dwarfs presented herein.

Our observing strategy is very similar to that described in Ibata et al. (2007), to which we refer the reader for further details. In brief, CFHT/MegaPrime consists of a mosaic of 36 2048 $\times$ 4612 pixel CCDs with a total field of view of 0.96×0.94 deg^2 at a pixel scale of 0.187 arcsec pixel^{-1}. We observe in the CFHT g and i bands for a total of 1350 s each, split into 3×450 s dithered subexposures, in $<0.8''$ seeing. This is sufficient to reach $g \sim 25.5$ and $i \sim 24.5$ with a signal-to-noise ratio of 10. In some cases, more than three exposures were taken (at the discretion of CFHT staff to ensure the requested observing conditions were met), and in these cases the viable images were included in the stacking procedure, weighted according to noise/seeing. We have chosen a tiling pattern which typically has very little overlap between fields, and so we use short, 45 s exposures in g and i offset by half a degree in the right ascension and declination directions in order to establish a consistent photometric level over the survey. This typically has a rms scatter of 0.02 mag over our survey area.

The CFHT/MegaPrime data were preprocessed by CFHT staff using the Elixir pipeline, which accomplishes the bias, flat, and fringe corrections, and also determines the photometric zero point of the observations. These images were then processed using a version of the Cambridge Astronomical Survey Unit (CASU) photometry pipeline (Irwin & Lewis 2001) adapted for CFHT/MegaPrime observations. The pipeline includes reregistration, stacking, catalog generation, and object morphological classification, and creates band-merged g, i products for use in the subsequent analysis. The CFHT g and i magnitudes are dereddened using the Schlegel et al. (1998) *IRAS* maps, such that $g_0 = g - 3.793\,E(B-V)$ and $i_0 = i - 2.086\,E(B-V)$, where g_0 and i_0 are the dereddened magnitudes.

3. ANALYSIS

In this section we present an initial analysis of the three new dwarf galaxies using the CFHT/MegaPrime discovery data. The measured parameters of the dwarfs are summarized in Table 1.

3.1. *Discovery and Stellar Populations*

Two of the new dwarf galaxies (Andromeda XVIII and XIX) stand out as prominent overdensities of stars in our survey and can be clearly identified by eye in maps of the distribution of stellar sources. Andromeda XX, on the other hand, is considerably fainter, and its color-magnitude diagram (CMD) is far more sparsely populated. Despite this, it was initially identified by one of us (A. Huxor) through visual examination of the individual CCDs during a search for globular clusters. An automated detection algorithm, based on a boxcar matched-filter search for local overdensities with a variable width, was subsequently applied after these preliminary searches. As well as highlighting these three dwarfs, some other dwarf galaxy candidates were identified and are being followed up. A subsequent paper will deal in detail with the automated detection of dwarf galaxies around M31 to enable a full completeness study, although such an analysis requires more contiguous coverage of M31 than we currently possess. Prior to

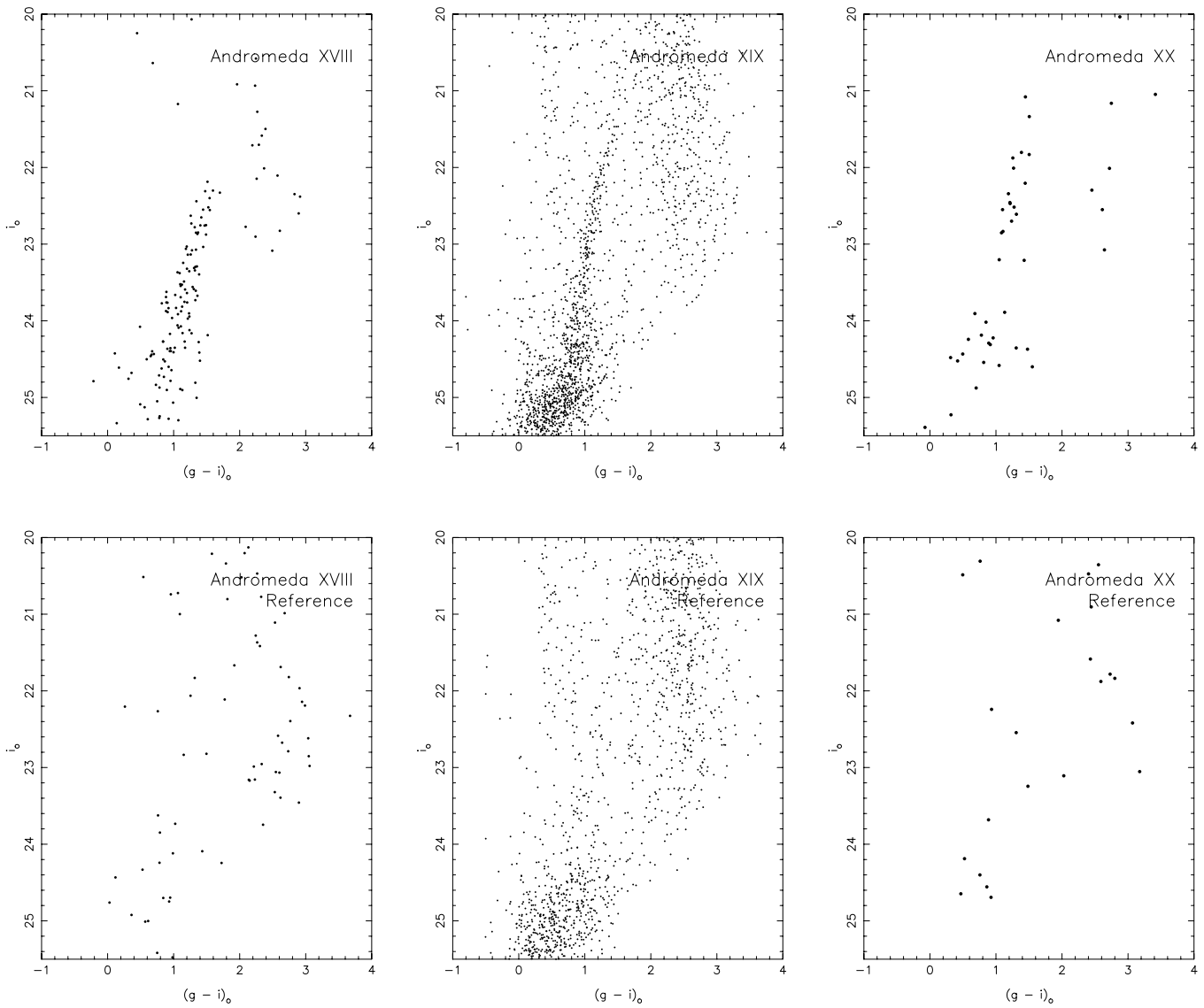

FIG. 2.—*Top panels*: Comparison of the i_0 vs. $(g-i)_0$ CMDs of the three newly discovered Local Group galaxies: Andromeda XVIII (*left*), XIX (*center*), and XX (*right*), where all stars lying within 2 half-light radii from the center of each galaxy have been plotted (corresponding to 1.8′, 12.4′, and 1′, respectively). *Bottom panels*: Reference fields probing an equivalent area offset from each galaxy by several half-light radii. A RGB is visible in each galaxy, although in the case of Andromeda XX it is very sparsely populated. None of the galaxies display any evidence for bright blue stars (either bright main sequence or blue loop), indicative of a young population, and in this respect they resemble the typical stellar populations of dSph galaxies. The faint blue objects centered around $i_0 \sim 25.2$ with a mean color of $(g-i)_0 \sim 0.5$ in the Andromeda XIX CMD may be a horizontal-branch component, although contamination from misidentified galaxies is considerable in this region of color-magnitude space.

such a study, we do not make any claims regarding the completeness of the satellite sample so far discovered.

The top panels of Figure 2 show the i_0 versus $(g-i)_0$ CMDs for the three new dwarf galaxies discovered in the southwest quadrant of M31 and whose positions relative to this galaxy are indicated in Figure 1. The bottom panels of Figure 2 show reference fields with equivalent areas offset from the center of each of the galaxies by several half-light radii. Each of the CMDs has been corrected for foreground extinction. In each of the three cases, a red giant branch (RGB) is clearly visible, although in the case of Andromeda XX it is poorly populated. To the depth of these observations, it appears that there are very few, if any, bright main-sequence and blue loop stars which would be indicative of younger stellar populations, and it is likely therefore that these galaxies do not host a dominant young population. Stars to the red of the RGB [with $2 \lesssim (g-i)_0 \lesssim 3$] are likely foreground Milky Way disk stars, although intermediate-age asymptotic giant branch stars can also occupy this color locus and have a luminosity similar to or brighter than the tip of the red giant branch (TRGB; although this is probably only relevant for Andromeda XIX). In the Andromeda XIX CMD and reference field, the vertical feature at $(g-i)_0 \sim 0.3$ is the foreground Milky Way halo locus (see Martin et al. [2007] for an analysis of this feature in our extant M31 survey). Given these current data, all of the CMDs appear to show stellar populations typical of dSph galaxies. The faint blue objects centered around $i_0 \sim 25.2$ with a mean color of $(g-i)_0 \sim 0.5$ in the Andromeda XIX CMD may be a horizontal-branch component. However, as the reference field shows, contamination from misclassified background galaxies is considerable in this region of color-magnitude space. There is also some evidence of a very weak RGB population in the Andromeda XIX reference field, which is likely due to the background M31 halo and stellar overdensities in the vicinity of this dwarf galaxy (see § 4.3.2).

Figure 3 shows various properties for each of the three new dwarf galaxies. The leftmost panels show I_0 versus $(V-I)_0$

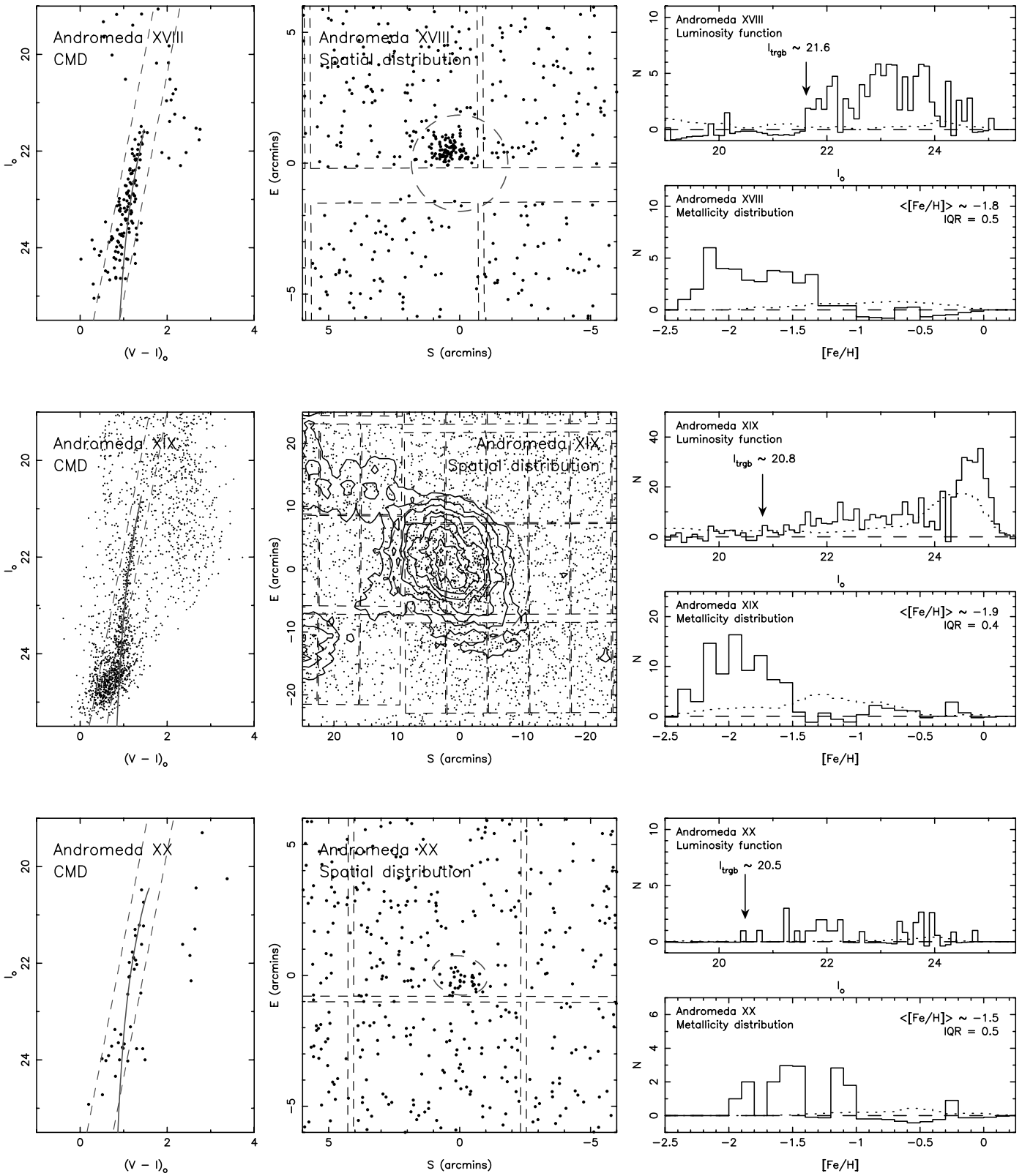

FIG. 3.—Various properties of Andromeda XVIII (*top row*), Andromeda XIX (*middle row*), and Andromeda XX (*bottom row*). *Left panels*: I_0 vs. $(V-I)_0$ CMD for each galaxy. Dashed lines define a color cut used to preferentially select stars associated with the dwarf. A 13 Gyr isochrone with the representative metallicity of the dwarf from VandenBerg et al. (2006) shifted to the appropriate distance modulus, is overlaid on each CMD. Only stars within the dotted ellipses shown in the center panels are plotted. *Center panels*: Tangent plane projections of the spatial distribution of stars in the vicinity of each dwarf. Only stars satisfying the color cuts shown in the CMDs are plotted. Dashed lines show the edges of the CFHT/MegaPrime CCDs. Dashed ellipses mark 2 half-light radii from the center of each galaxy. For Andromeda XVIII and XX, the dwarf galaxies are clearly visible as overdensities in the centers of each field, whereas Andromeda XIX is more extended and diffuse, and contours have been overlaid to more clearly define its structure. The first contour is set 3 σ above the background, and subsequent contour levels increase by 1.5 σ over the previous level. *Right top panels*: foreground-corrected, dereddened, *I*-band luminosity functions of stars in each galaxy satisfying our color and spatial cuts. Scaled reference field luminosity functions are shown as dotted lines. The estimated luminosity of the TRGB is highlighted. *Right bottom panels*: Foreground-corrected observed photometric MDF derived using the technique detailed in McConnachie et al. (2005) using 13 Gyr isochrones from VandenBerg et al. (2006) with $[\alpha/\mathrm{Fe}] = 0$. Scaled reference field MDFs are shown as dotted lines. The mean metallicity and metallicity spread (quantified using the IQR) for each galaxy is highlighted. [*See the electronic edition of the Journal for a color version of this figure.*]

CMDs for each galaxy. We have transformed CFHT *gi* to Landolt *VI* using a two-stage transformation; we first change CFHT *gi* into INT $V'i$ using the relations derived in Ibata et al. (2007), and we then transform INT $V'i$ into Landolt *VI* using the transformations given in McConnachie et al. (2004).[10] In each CMD, only those stars which lie within 2 half-light radii from the center of each galaxy (shown by the dashed ellipse in the second panel) have been plotted. The dashed lines define a color cut designed to preferentially select stars which are members of the dwarf galaxies. The solid line shows a 13 Gyr isochrone with the representative metallicity of the dwarf from VandenBerg et al. (2006) shifted to the distance modulus of the dwarf (the distance and metallicity of each dwarf is calculated in § 3.2).

The second panel in each row of Figure 3 shows the spatial distribution of candidate RGB stars in the vicinity of each galaxy, defined by the color cuts discussed previously. Dashed lines show the edges of the CFHT/MegaPrime CCDs. Both Andromeda XVIII and XX appear as obvious concentrations of stars, despite Andromeda XX being poorly populated. Andromeda XVIII lies at the corner of one of the CCDs, and much of this galaxy hides behind the large gap between the second and first rows of CCDs in the CFHT/MegaPrime field (see § 3.3). Andromeda XIX is a much more extended and diffuse system than the other two, and contours have been overlaid to more clearly show its structure. The first contour is set 3 σ above the background, and subsequent contour levels increase by 1.5 σ over the previous level. This galaxy is located on the boundary of our survey, overlapping slightly with the extant survey region from Ibata et al. (2007). We include some adjacent fields from this earlier part of the survey to obtain complete coverage of Andromeda XIX.

3.2. *Distances and Metallicities*

The upper right panels in each row of Figure 3 show, for each galaxy, the dereddened *I*-band luminosity functions of stars in the CMD which satisfy the color and spatial cuts defined previously. These have been corrected for foreground/background contamination by subtracting a nearby "reference" field, scaled by area. The scaled reference field is shown by the dotted line, to illustrate the contribution from the foreground/background as a function of magnitude. The *I*-band magnitude of the TRGB (corresponding to the point in the evolution of a RGB star immediately prior to it undergoing the core helium flash) is a well-calibrated standard candle which is used extensively for nearby galaxies (e.g., Lee et al. 1993; Salaris & Cassisi 1997; McConnachie et al. 2004, 2005 and references therein). In a well-populated luminosity function, it is normally taken to be equal to the luminosity of the brightest RGB star. However, when dealing with faint dwarfs—particularly systems like Andromeda XX with a very sparse RGB—this assumption is likely to be flawed due to sampling errors. However, for this initial analysis of these galaxies we assume that the TRGB position measured in this way is a good estimate of its actual position. We note that the resulting distance modulus of Andromeda XX in particular is uncertain and will be refined once deeper data reaching below the horizontal branch are available.

Our best estimates for the (extinction corrected) *I*-band magnitude of the TRGB are highlighted on each of the luminosity functions in Figure 3 and are listed in Table 1. For Andromeda XX, we have adopted very conservative error bars; the lower limit is an estimate of the possible offset of the brightest RGB star from the true TRGB from our experience with the comparably faint Andromeda XII (Chapman et al. 2007); the upper limit assumes

[10] See http://www.ast.cam.ac.uk/~wfcsur for details.

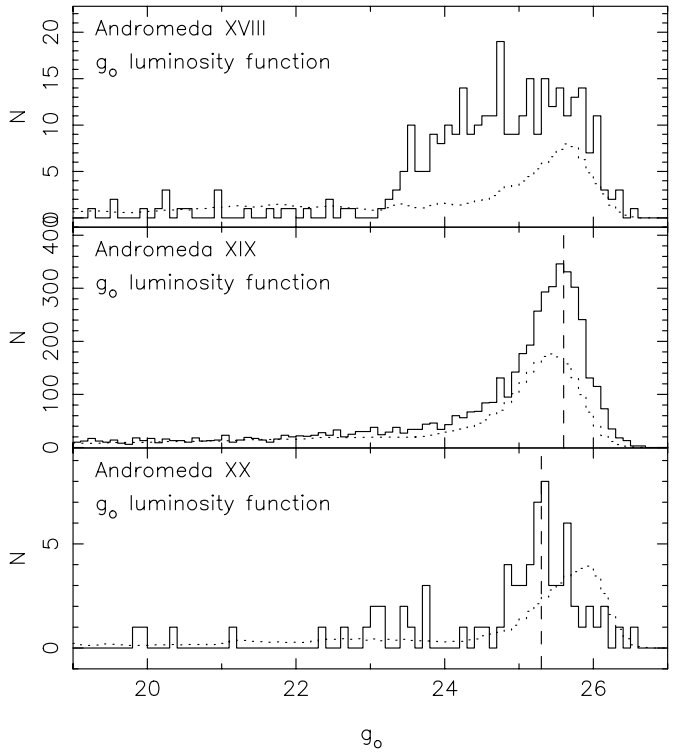

FIG. 4.—Dereddened *g*-band luminosity functions of stars within 2 half-light radii of Andromeda XVIII, XIX, and XX (*top, middle, and bottom panels, respectively*). These luminosity functions go deeper than the CMDs shown previously, since only detection in the *g* band is required. Nearby reference fields, scaled by area, are shown as dotted lines in each panel. For reference, the horizontal branch of M31 has a magnitude of $g_0 \sim 25.2$. In Andromeda XIX and XX, we attribute the peak of stars at $g_0 \sim 25.3$ and $g_0 \sim 25.6$, respectively, to a detection of horizontal-branch stars (*dashed lines*). In Andromeda XVIII, no feature attributable to the horizontal branch is visible, as expected from its larger distance. Thus, these detections (and nondetection) are consistent with the distances derived for these galaxies via the TRGB analysis.

that the few brightest stars we have identified are actually foreground contamination, and that the true TRGB is represented by the group of stars at $I_0 \sim 21.2$. Adopting $M_I = -4.04 \pm 0.12$ (Bellazzini et al. 2001) yields a preliminary distance to each of the new dwarf galaxies; the derived distance moduli and distances are given in Table 1. Most notable is the distance to Andromeda XVIII, which has a well-defined TRGB, and which places it approximately 1.4 Mpc from the Milky Way (~600 kpc distant from M31), at the periphery of the Local Group.

As an independent check of our distance estimates (particularly that for Andromeda XX), we construct g_0 luminosity functions for each galaxy using stars within 2 half-light radii of the centers. These are shown in Figure 4 as solid lines. Also shown as dotted lines are luminosity functions for nearby reference fields, scaled by area. These luminosity functions go deeper than the previous CMDs, since stars are only required to be detected in the *g* band. Our data start to become seriously incomplete below $g_0 \sim 25.5$, and photometric errors at this magnitude are of order $\Delta g \simeq 0.15$. For reference, the horizontal branch in M31 has a magnitude of $g_0 \sim 25.2$ (Ibata et al. 2007). For Andromeda XIX and XX, peaks of stars are visible at $g \sim 25.3$ and $g \sim 25.6$, respectively, which are not present in the reference fields, and which are marked in Figure 4 by dashed lines. We attribute these peaks to the detection of horizontal-branch stars in each of these galaxies. While the peak for Andromeda XIX is less apparent than that for Andromeda XX, its position coincides with the expected luminosity of the horizontal branch from inspection of its

CMD in Figure 2, reinforcing our interpretation of this feature. In contrast, no such feature is visible for Andromeda XVIII, which is expected given that we measure it to be much more distant than the other two, and so our observations will not be deep enough to observe the horizontal-branch population. Similarly, our measurements of the positions of the horizontal branches in Andromeda XIX and XX are consistent with the positions we measure for the TRGB in these galaxies. These detections (and nondetection) of the horizontal branches are therefore consistent with the distances derived from the TRGB, and suggest that the uncertainty in the distance to Andromeda XX may be less than we currently adopt in Table 1.

The lower right panels of Figure 3 show the observed photometric metallicity distribution function (MDF), constructed using the same technique as detailed in McConnachie et al. (2005) using a bilinear interpolation of stars in the top two magnitudes of the RGB with 13 Gyr isochrones, $[\alpha/\mathrm{Fe}] = 0$, from VandenBerg et al. (2006) with *BVRI* color-T_{eff} relations as described by VandenBerg & Clem (2003). Each MDF has been corrected for foreground/background contamination by subtraction of a MDF for a reference field, scaled by area. The MDF for the scaled reference field is shown as a dotted line in each panel. The mean metallicity and metallicity spread, as quantified by the interquartile range (IQR), are highlighted in Figure 3, and an isochrone corresponding to the mean metallicity of the dwarf is overlaid on the CMD in the first panels, shifted to the distance modulus of the dwarf galaxy.

The metallicity spread in each of the three galaxies is similar, although the IQR for Andromeda XIX appears slightly smaller than for the other two. Certainly, the color spread of the RGB seen from the CMDs is much smaller for Andromeda XIX than for Andromeda XVIII and XX. That this does not correspond to a much smaller spread in metallicity probably reflects the metal-poor nature of Andromeda XIX, since RGB color is a poor indicator of metallicity variation at very low metallicities. It is also tempting to suggest that the narrow spread in RGB color indicates that Andromeda XIX is a simple stellar population; however, lessons learned from the Carina dSph, which has a large age and metallicity spread but conspires to have a narrow RGB (Smecker-Hane et al. 1994), suggest a note of caution against this interpretation.

The metallicity information is summarized in Table 1. The formal uncertainties in the metallicity and metallicity spread estimates are of order 0.1 dex. In addition to uncertainties in the stellar models, our metallicity estimates assume that (1) the dwarfs are all dominated by a 13 Gyr stellar population, and (2) the distance modulus for each galaxy is well estimated. The former assumption is likely reasonable, and should not lead to an error $\gtrsim$0.2 dex unless the dwarfs are dominated by intermediate-age and young stellar populations (for which there is no current evidence). The latter assumption looks to be reasonable for Andromeda XVIII and XIX, where the RGB is reasonably well populated, but for Andromeda XX the uncertainty introduced through the distance estimate could be more significant. We note that the metallicities of Andromeda XVIII and XIX look to be significantly lower than the median metallicity of the kinematically selected halo of M31, which has $[\mathrm{Fe/H}] \simeq -1.4$ (Chapman et al. 2006; Kalirai et al. 2006).

3.3. *Structures and Magnitudes*

We quantify the structures of Andromeda XVIII, XIX, and XX through the spatial distributions of their resolved stars. However, the analysis is made more complex since Andromeda XIX is very diffuse, Andromeda XX has very few bright stars on which to base our analysis, and each of the dwarf galaxies lies close to or at the edges of CCDs. In the extreme case of Andromeda XVIII, we are clearly missing a significant part of the galaxy which lies behind the large gap between the second and first rows of the CFHT/MegaPrime mosaic. To illustrate this, the top panel of Figure 5 shows the *i*-band image of Andromeda XVIII with linear scaling; while Andromeda XVIII is clearly visible to the naked eye, much of the galaxy falls off the edge of the detector. To determine how large this effect is, the bottom panel of Figure 5 shows a $10' \times 10'$ image centered on the coordinates of Andromeda XVIII from the POSS II United Kingdom Schmidt Telescope Unit (UKSTU)

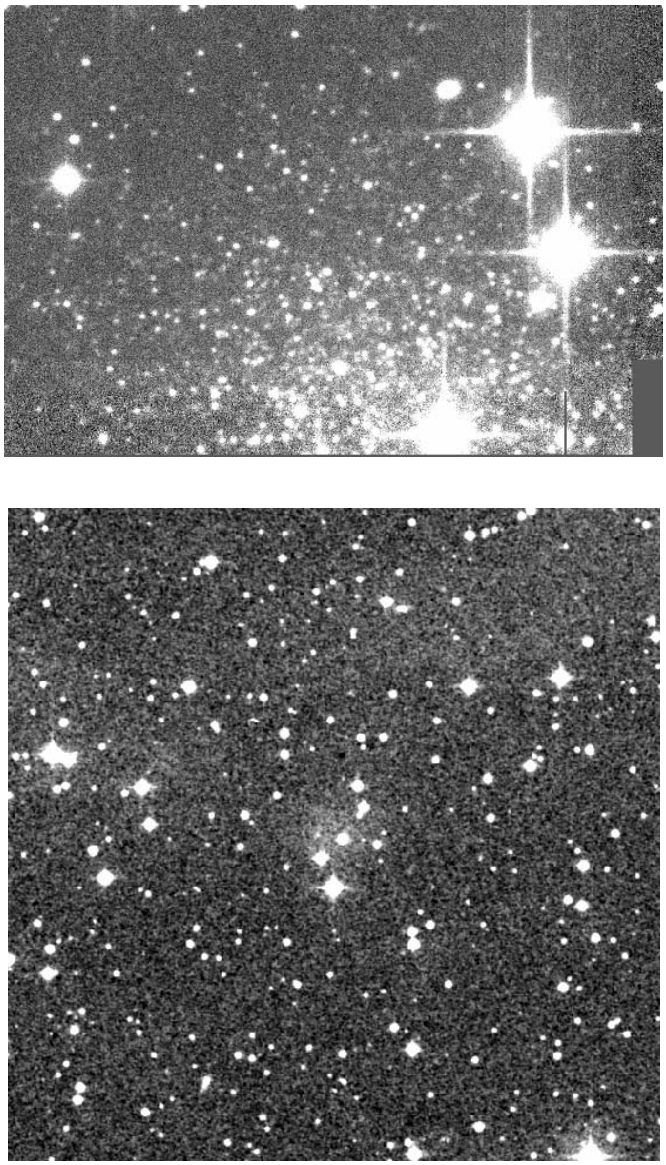

FIG. 5.— *Top*: The CFHT/MegaPrime *i*-band image of Andromeda XVIII with linear scaling. Approximately $2.5' \times 1.2'$ in the vicinity of Andromeda XVIII is shown. This galaxy lies in the southwest corner of one of the CCDs, and some of it remains hidden behind the large gap between the second and first rows of CFHT/MegaPrime mosaic. Unlike the majority of recent discoveries in the Local Group, Andromeda XVIII is clearly visible based on its resolved light. *Bottom*: A $10' \times 10'$ image centered on the coordinates of Andromeda XVIII, with linear scaling, from the POSS II/UKSTU (Blue) survey, taken from the DSS. Andromeda XVIII is visible at the center. Some Galactic nebulosity is also present in this region. This galaxy is also visible on the original POSS I (Blue) survey plates, and suggests that there may be other comparably bright galaxies within the Local Group which have so far eluded detection. In each panel, north is up, and east is to the left.

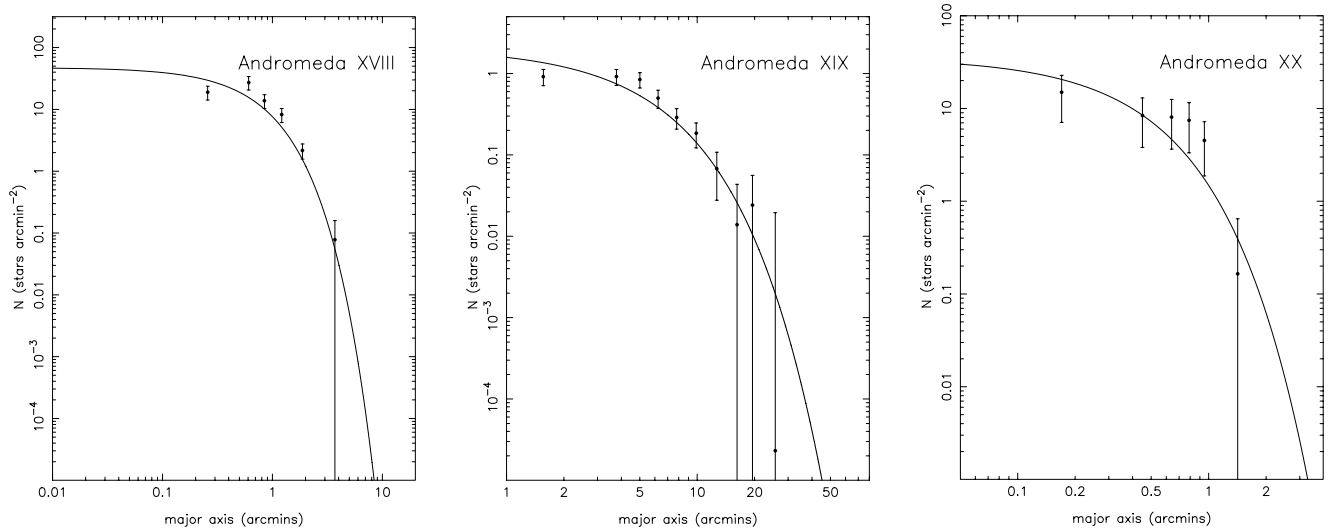

FIG. 6.—Radial profiles of Andromeda XVIII, XIX, and XX (*left to right, respectively*), derived in the same way as in McConnachie & Irwin (2006a) using elliptical annuli with the position angles, ellipticities, and centroids listed in Table 1. Overlaid on these profiles are the most probable exponential profiles derived using the same maximum likelihood technique.

(Blue) survey which we retrieved through the DSS, and which covers the entirety of this galaxy.

Given the several complications discussed above, we choose to derive the structural parameters for the dwarfs based on the maximum likelihood technique developed by Martin et al. (2008) instead of the usual technique, which bins the data spatially and uses smoothing kernels (e.g., Irwin & Hatzidimitriou 1995; McConnachie & Irwin 2006a). The procedure has been modified from Martin et al. (2008), to which we refer the reader for details, to account for incomplete coverage of the dwarfs due to CCD edges. In brief, this technique calculates simultaneously the most plausible values for the centroid, ellipticity, position angle, and half-light radius of the dwarf under the assumption that the surface brightness radial profile is well described by an exponential curve, without any need for smoothing or binning of the data. However, for Andromeda XVIII this approach is still insufficient, since our data only sample one segment of the galaxy, as shown by comparing the POSS II/UKSTU image with the CFHT/MegaPrime image in Figure 5. Thus, for this galaxy, we estimate its center from the POSS II/UKSTU data and approximate it as circular. The half-light radius is then calculated via the same technique as for Andromeda XIX and XX using the CFHT/MegaPrime data.

The centroid, half-light radius (r_h), position angle (measured east from north), and ellipticity ($\epsilon = 1 - b/a$) for each dwarf galaxy, derived using the maximum likelihood technique (with the above caveat for Andromeda XVIII), are listed in Table 1. In addition, Figure 6 shows the (background corrected) stellar density profile (equivalent to the surface brightness profile), derived using the same technique as in McConnachie & Irwin (2006a) for each of the three dwarf galaxies. We use elliptical annuli with the position angle, ellipticity, and centroid listed in Table 1. Overlaid on these profiles are exponential profiles with the appropriate half-light radii (the exponential scale radius, $r_e \simeq 0.6 r_h$). These profiles are the most probable exponential models for the stellar density distribution of the dwarf galaxy derived using the maximum likelihood method, and are not fits to the averaged data points.

We estimate the magnitude of Andromeda XIX and XX in a similar way as Martin et al. (2006) and Ibata et al. (2007). First, we sum the total *V*-band flux from candidate member stars which are within the half-light radius of each dwarf galaxy and which are within 2–3 mag of the TRGB. However, this flux does not take into account the contribution to the total light from fainter stars, most of which we do not detect. To determine the appropriate correction to apply, we compare the half-light flux of Andromeda III measured in this way (using similar CFHT/MegaPrime observations) to its apparent magnitude of $m_v = 14.4 \pm 0.3$, directly measured by McConnachie & Irwin (2006a). We then apply the appropriate correction to the fluxes for each dwarf galaxy. Clearly, the uncertainties associated with this method are considerable, and we make the implicit assumption that the luminosity functions of Andromeda III, XIX, and XX are similar. Under this assumption, we estimate an accuracy of $\sim$0.6 mag in the final magnitude of Andromeda XIX, although we estimate a larger uncertainty of $\sim$0.8 mag for Andromeda XX due to the small number of bright stars available. The central surface brightness of Andromeda XIX and XX are estimated by normalizing the exponential profiles shown in Figure 6, so that the surface integral over the dwarf out to the half-light radius is equal to half the total flux received from the dwarf. These numbers are also given in Table 1.

It is not possible to derive the magnitude of Andromeda XVIII in the same way as above, given that we only sample a segment of this galaxy with our data. Comparison of the POSS II/UKSTU images of Andromeda XVIII with those of Andromeda V, VI, and VII show that it is considerably lower surface brightness than either Andromeda VI or VII, but is similar to—and perhaps brighter than—that of Andromeda V, which has $S_0 = 25.6 \pm 0.3$ (McConnachie & Irwin 2006a). We therefore adopt this as a faint-end limit to the central surface brightness of Andromeda XVIII. A faint-end limit to its magnitude can then be calculated by normalizing its radial surface brightness profile to this central value, integrating over its area out to the half-light radius, and multiplying the answer by 2. The magnitude derived in this way is given in Table 1. We note that updated magnitudes and surface brightnesses will be derived for each of the three new galaxies using the unresolved light component from dedicated, follow-up, photometric studies.

4. DISCUSSION

Andromeda XVIII, XIX, and XX have a range of relatively unusual properties. In particular, Andromeda XVIII is one of the

most distant Local Group galaxies discovered for several years, and is one of the most isolated systems in the Local Group. Andromeda XIX is extremely extended, with a very large half-light radius and extremely faint central surface brightness. Andromeda XX, on the other hand, is one of the lowest luminosity dwarf galaxies so far discovered around M31, with a magnitude of $M_V \simeq -6.3^{+1.0}_{-0.7}$, comparable to the luminosity of Andromeda XII ($M_V = -6.4 \pm 1.0$; Martin et al. 2006). In this section, we discuss the properties of these galaxies in the larger context of the main science questions raised by the recent discoveries of so many new dwarf galaxies.

4.1. *Completeness*

Prior to 2004, there were 17 dSph galaxies known in the Local Group (nine Milky Way satellites, six M31 satellites; and two isolated systems: Cetus and Tucana). Since this time, 23 new dwarf galaxies (including possible diffuse star clusters around the Milky Way) have been discovered in the Local Group, the overwhelming majority of which are dSph satellites of the Milky Way and M31. For the Milky Way, the SDSS has been responsible for all the discoveries to date, and most of the galaxies discovered have been extremely faint; no new Milky Way satellites with $M_V \lesssim -8$ have been found. Thus, apart from satellites hidden by the Milky Way disk, our satellite system is probably complete to this approximate magnitude limit, as originally argued by Irwin (1994).

Around M31, it is more difficult to identify extremely faint dwarf galaxies, since we cannot probe as far down the stellar luminosity function. Andromeda XII and Andromeda XX are the two faintest M31 satellites found so far, both with $M_V \sim -6.3$. For comparison, the faintest Milky Way satellite found to date is probably Willman I, with $M_V \sim -2.7$ (Willman et al. 2006; Martin et al. 2008).

Andromeda XVIII is considerably brighter than Andromeda XX, and has a central surface brightness similar to or brighter than Andromeda V ($S_0 = 25.6 \pm 0.3$ mag arcsec^{-2}). Andromeda XVIII is clearly visible in the POSS II/UKSTU (Blue) survey image, which we retrieved through the DSS and which is reproduced in the lower panel of Figure 5. However, its identification is made more complicated by numerous nearby bright stars and nebulosity in its vicinity, which may act to explain why it was not discovered using these data. We have also confirmed that it is visible in the original POSS I (Blue) survey. Its belated discovery indicates that previous surveys for relatively *bright* dwarf galaxies around M31 were incomplete and that some dwarfs were missed. Variable and unknown completeness is problematic for studies of satellite distributions, and highlights the vital need for more systematic studies such as those now being conducted.

It is fortuitous that Andromeda XVIII lies within our survey area given its considerable distance from M31. Indeed, even as current and future surveys help improve the completeness of the M31 and Milky Way satellite systems, many isolated Local Group galaxies can be expected to continue to elude detection: unlike the Milky Way satellites, they are not nearby, and unlike the M31 satellites, they are not necessarily clustered in an area amenable to systematic searches. PanStarrs 3π will survey a large fraction of the sky a magnitude deeper than SDSS, and should discover isolated Local Group galaxies, particularly those within 500 kpc or so from the Milky Way. However, very faint galaxies much farther away than this ($\sim$1 Mpc) may prove more difficult to spot. Exactly how many very faint dwarf galaxies are to be found at the periphery of the Local Group is likely to remain uncertain for some time yet.

4.2. *Spatial Distribution*

Several recent studies of the spatial distributions of satellites around the Milky Way and M31 (Willman et al. 2004; Kroupa et al. 2005; McConnachie & Irwin 2006b; Koch & Grebel 2006; Metz et al. 2007; Irwin et al. 2008) have generally concluded that the distributions appear anisotropic: McConnachie & Irwin (2006b) highlight the fact that (at the time) 14 out of the 16 candidate satellites of M31 are probably on the near side of M31, while others (Kroupa et al. 2005; Koch & Grebel 2006; Metz et al. 2007; Irwin et al. 2008) conclude that many of the Milky Way and M31 satellites are aligned in very flattened, disklike, distributions (an observation originally made by Lynden-Bell [1976, 1982]).

Andromeda XVIII, XIX, and XX do not lie near any of the principle satellite planes previously proposed to exist around M31. As discussed in the previous subsection, the census of Local Group galaxies is clearly not complete, and it is too early to draw definitive conclusions regarding the distributions of satellites. This is particularly true around M31, where relatively bright satellites are still being discovered. For the Milky Way, the SDSS covers roughly one-fifth of the Milky Way halo in the direction of the north Galactic cap; depending on how many satellites are found in future surveys at lower latitudes, the statistical significance of the proposed streams of satellites may change substantially.

In terms of spatial distributions, Andromeda XVIII is unusual, insofar as it is very distant—roughly 1.4 Mpc from the Milky Way, and roughly 600 kpc from M31. Thus, it is probably not a satellite of M31, although kinematics may help reveal whether it is approaching M31 and the Local Group for the first time (like Andromeda XII; Chapman et al. 2007), or if it has been thrown out from M31 following an interaction (like Andromeda XIV: Majewski et al. 2007; Sales et al. 2007).

4.3. *Environment and Structures*

4.3.1. *Andromeda XVIII, Position and Morphology*

Andromeda XVIII appears to possess stellar populations typical of dSph galaxies. If it is subsequently confirmed to be gas-poor, then it will be the third dSph galaxy found in isolation in the Local Group (in addition to Cetus and Tucana). The fact that isolated galaxies are preferentially more gas-rich compared to satellites (Einasto et al. 1974) has led to the proposition that satellite galaxies are stripped of their gas via ram pressure stripping and tidal harassment in the halo of the host galaxy (e.g., Mayer et al. 2006). However, for isolated systems such as Andromeda XVIII, Cetus, and Tucana, prolonged interactions with massive galaxies are unlikely to have occurred. Likewise, the gas-deficient satellite Andromeda XII is not believed to have undergone any past interactions with a large galaxy, since it appears to be on its first infall into the potential of M31 (Chapman et al. 2007). Furthermore, the most compelling case of a dwarf galaxy thought to be undergoing ram pressure stripping is Pegasus (DDO 216; McConnachie et al. 2007b), an *isolated* galaxy more than 400 kpc from M31. Clearly, understanding if these observations are consistent with the present models for dwarf galaxy evolution requires a more complete inventory of nearby galaxies and their properties than we currently possess.

4.3.2. *Andromeda XIX, Tides and Substructure*

The half-light radius of Andromeda XIX is $6.2'$. At the distance we derive for it, this corresponds to $r_h \simeq 1.7$ kpc, which is the largest value yet recorded for any dSph in the Local Group. The average half-light radius for Milky Way dSphs is an order of

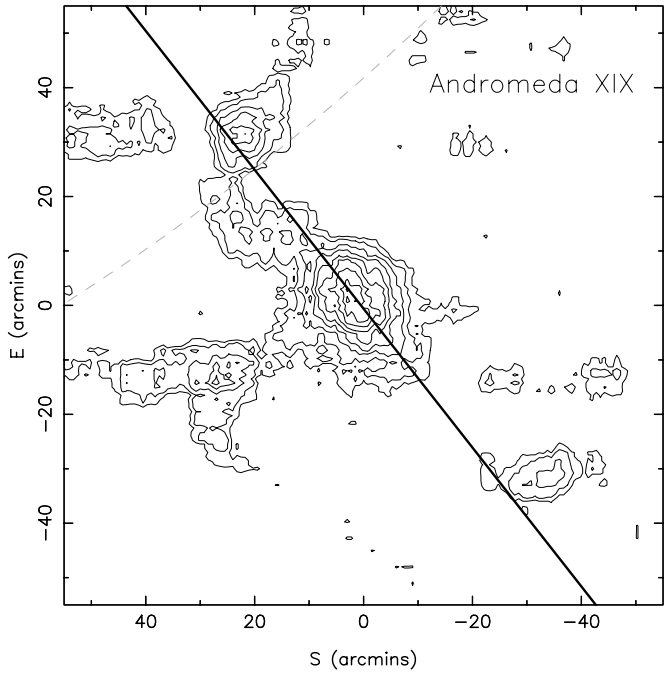

FIG. 7.— Surroundings of Andromeda XIX, shown as a tangent plane projection of the stellar density. The first two contour levels are 2 and 3 σ above the background, and then they increase by 1.5 σ over the previous level. The major axis of M31 is shown as the solid line, and the dashed line shows part of the circle which marks the 100 kpc boundary from the center of M31, as in Fig. 1. Andromeda XIX lies close to the major-axis substructure identified in Ibata et al. (2007), some of which can be seen in this plot. There is also some evidence of tidal features in the outskirts of Andromeda XIX. [*See the electronic edition of the Journal for a color version of this figure.*]

magnitude less, at $r_h \sim 150$ pc, and none have half-light radii larger than $r_h \simeq 550$ pc (with the exception of the tidally disrupting Sagittarius dSph; Majewski et al. 2003). M31 dSphs, on the other hand, have typical half-light radii of $r_h \sim 300$ pc, with the previous extremes being Andromeda II, with $r_h \simeq 1.1$ kpc, and Andromeda VII, with $r_h \simeq 750$ pc (McConnachie & Irwin 2006a). The extremely diffuse and extended nature of Andromeda XIX is reminiscent of the "outer component" of Andromeda II, as traced by horizontal-branch stars by McConnachie et al. (2007a).

It is tempting to attribute the diffuse structure of Andromeda XIX to tidal interactions. In this respect, it is relevant to note that Andromeda XIX lies very close to the major-axis substructure identified by Ibata et al. (2007). No independent distance estimate to this substructure currently exists; Ibata et al. (2007) assumed it to be at the distance of M31, but if it is at the same distance as Andromeda XIX, then the photometric metallicity estimates of these features will be very similar. Figure 7 shows the surroundings of Andromeda XIX as a stellar density map; the first two contour levels are 2 and 3 σ above the background, and the levels then increase by 1.5 σ over the previous level. As well as showing Andromeda XIX as a prominent overdensity, there is some evidence of stellar material in its outskirts (also visible in the contours of Fig. 3). Whether or not Andromeda XIX is the source of the major-axis substructure identified in Ibata et al. (2007) or is being tidally perturbed, will require detailed kinematics in this region. We note that Peñarrubia et al. (2008b) show that the effect of tides on dwarf galaxies in cosmological halos is to decrease the central surface brightness and *decrease* the half-light radius of the bound component. This would argue against tidal effects explaining the structure of Andromeda XIX.

The large-scale size of Andromeda XIX reinforces the difference in scale size between the Milky Way and M31 satellites first highlighted in McConnachie & Irwin (2006a), such that the M31 dSphs are more extended than their Milky Way counterparts. Peñarrubia et al. (2008a, 2008b) have investigated the cause of this disparity in an attempt to relate it to either differences in the underlying dark matter properties of the dwarfs or differences in their evolution around their hosts. They conclude that tidal effects are insufficient to explain the magnitude of the effect. However, if the different scale sizes reflect intrinsic differences between the Milky Way and M31 subhalos, then this should reveal itself in the kinematics of the two populations (with the M31 dwarfs being dynamically hotter than their Milky Way counterparts). Whatever the cause, the comparison of Andromeda XIX and the other M31 satellites to the Milky Way population highlights the importance of sampling dwarfs in a range of environments so as to obtain a fuller appreciation of the range of properties that these systems possess. In turn, this helps us understand the physical drivers behind the differences and similarities we observe. We note that studies of the star clusters of M31 (Huxor et al. 2005, 2008) have already extended the known parameter space for these objects, with the M31 population containing extended star clusters not found in the Milky Way population.

4.4. *Satellites That are Missing and "the Missing Satellites"*

Andromeda XX is an exceptionally faint galaxy with a very poorly populated RGB. This makes an accurate derivation of its properties particularly difficult. However, the star formation history of Andromeda XX and the other ultrafaint satellites is particularly relevant to the "missing satellites" question: Do all the thousands of dark matter subhalos predicted to exist in the halos of galaxies like the Milky Way and M31 contain stars, and if they do, where are they? Until recently, only a dozen or so dwarf satellites were observed, and it was noted that the cumulative mass distribution of these satellites was dramatically different from that of predicted dark matter subhalos, even at relatively large masses (Moore et al. 1999; Klypin et al. 1999). To solve this discrepancy without altering the underlying cosmology, it was suggested that either there were a large number of luminous satellites awaiting discovery, or that not all subhalos have a luminous component.

Despite many new galaxies in the Local Group being discovered, and many more undoubtedly awaiting discovery, we consider it very unlikely that these discoveries will resolve the discrepancy between theory and observation. The original comparison between the observed and predicted satellite mass functions shows that the discrepancy sets in for dwarfs as luminous as the Small Magellanic Cloud ($M_V \simeq -16$) and Fornax ($M_V \simeq -13$). Finding thousands of very faint (and presumably less massive?) satellites would not solve the disagreement at the more massive end, and there is no evidence to suggest that a dozen galaxies with luminosity similar to Fornax have been missed (e.g., Irwin 1994). Furthermore, as higher resolution dark matter simulations make clear (e.g., Diemand et al. 2007), the subhalo mass function appears to continue to increase at the low-mass end. It seems reasonable, therefore, that at some point these halos will not be massive enough to be able to accrete and/or retain baryons and form stars, and this implies that there is a minimum mass halo which can host a luminous component (Kravtsov et al. 2004).

A reanalysis of the observed dynamics of the dwarf galaxies by Peñarrubia et al. (2008a, 2008b) within the ΛCDM framework has shown that few—if any—of these galaxies (including

recent discoveries) occupy a halo with a circular velocity less than $\sim$10–20 km s^{-1}. Furthermore, these estimates bring the cumulative distribution of luminous satellites and dark matter subhalos into good agreement at the high-mass end. Using a different technique, Strigari et al. (2007a) find a similar result. Given that these authors find good agreement between observations and theory down to a certain mass limit, their results support the idea of a mass threshold in dark matter halos below which star formation becomes highly inefficient. Therefore, by continuing to identify new, ultrafaint dwarfs, we probe the astrophysics of galaxy formation at low-mass limits where the sensitivity to complex feedback mechanisms—such as star formation (Kravtsov et al. 2004) and reionization (Bullock et al. 2001)—is greatest.

5. SUMMARY

We have presented three new Local Group dwarf galaxies discovered as part of our ongoing CFHT/MegaPrime survey of M31 and its environs. These galaxies—christened Andromeda XVIII, XIX, and XX after the constellation in which they are found—have stellar populations which appear typical of dSph galaxies. Individually, each of these galaxies has relatively unusual properties compared to the previously known dwarfs in the vicinity of M31:

1. Andromeda XVIII is extremely distant, at 1355 ± 88 kpc from the Milky Way, placing it nearly 600 kpc from M31. Thus, it is one of the most isolated galaxies in the Local Group. It is clearly observed through its integrated light (it appears to have a central surface brightness similar to or brighter than that of Andromeda V) and suggests that there could be several other relatively bright dwarf galaxies within the Local Group which have so far eluded detection;

2. Andromeda XIX is extremely extended, with a half-light radius of $r_h = 1683 \pm 113$ kpc. This is an order of magnitude more extended than typical Milky Way dSphs. While its integrated luminosity is $M_V = -9.3 \pm 0.6$, its central surface brightness is exceptionally low, at $S_0 = 29.3 \pm 0.7$. Andromeda XIX reinforces the difference in scale size between the Milky Way and M31 satellites first discussed in McConnachie & Irwin (2006a). This galaxy may be being tidally disrupted, and could be related to the major-axis substructure first identified in Ibata et al. (2007) and which lies near to Andromeda XIX in projection. However, we note that calculations by Peñarrubia et al. (2008b) show that the net effect of tides on a dwarf galaxy is to decrease the central surface brightness and *decrease* the half-light radius of the bound component;

3. Andromeda XX is extremely faint, with an absolute magnitude of order $M_V = -6.3^{+1.0}_{-0.7}$. It is one of the faintest galaxies so far discovered in the vicinity of M31 (comparable in luminosity to Andromeda XII), and as such many of its key parameters are extremely uncertain at this stage. A full inventory of these systems is required to properly define the faint end of the galaxy luminosity function, and to determine where, if anywhere, we encounter a lower limit to the galaxy mass/luminosity function.

Based on observations obtained with MegaPrime/MegaCam, a joint project of CFHT and CEA/DAPNIA, at the Canada-France-Hawaii Telescope (CFHT), which is operated by the National Research Council (NRC) of Canada, the Institute National des Sciences de l'Univers of the Centre National de la Recherche Scientifique of France, and the University of Hawaii. We are indebted to the CFHT staff for their help and careful observations, and we thank the anonymous referee for useful comments which improved the clarity of this paper. A. W. M. thanks Evan Skillman, Jorge Peñarrubia, and Andrew Cole for useful discussions. A. W. M. is supported by a Research Fellowship from the Royal Commission for the Exhibition of 1851, and thanks Sara Ellision and Julio Navarro for additional financial assistance. A. H. and A. M. N. F. acknowledge support from a Marie Curie Excellence Grant from the European Commission under contract MCEXT-CT-2005-025869.

REFERENCES

Armandroff, T. E., Davies, J. E., & Jacoby, G. H. 1998, AJ, 116, 2287
Armandroff, T. E., Jacoby, G. H., & Davies, J. E. 1999, AJ, 118, 1220
Bellazzini, M., Ferraro, F. R., & Pancino, E. 2001, ApJ, 556, 635
Belokurov, V., et al. 2006, ApJ, 647, L111
———. 2007, ApJ, 654, 897
Bullock, J. S., Kolatt, T. S., Sigad, Y., Somerville, R. S., Kravtsov, A. V., Klypin, A. A., Primack, J. R., & Dekel, A. 2001, MNRAS, 321, 559
Bullock, J. S., Kravtsov, A. V., & Weinberg, D. H. 2000, ApJ, 539, 517
Chapman, S. C., Ibata, R., Lewis, G. F., Ferguson, A. M. N., Irwin, M., McConnachie, A., & Tanvir, N. 2006, ApJ, 653, 255
Chapman, S. C., et al. 2007, ApJ, 662, L79
Dekel, A., & Silk, J. 1986, ApJ, 303, 39
Dekel, A., & Woo, J. 2003, MNRAS, 344, 1131
Diemand, J., Kuhlen, M., & Madau, P. 2007, ApJ, 667, 859
Einasto, J., Saar, E., Kaasik, A., & Chernin, A. D. 1974, Nature, 252, 111
Ferguson, A. M. N., Gallagher, J. S., & Wyse, R. F. G. 2000, AJ, 120, 821
Ferguson, A. M. N., Irwin, M. J., Ibata, R. A., Lewis, G. F., & Tanvir, N. R. 2002, AJ, 124, 1452
Gilmore, G., Wilkinson, M. I., Wyse, R. F. G., Kleyna, J. T., Koch, A., Evans, N. W., & Grebel, E. K. 2007, ApJ, 663, 948
Huxor, A. P., Tanvir, N. R., Ferguson, A. M. N., Irwin, M. J., Ibata, R., Bridges, T., & Lewis, G. F. 2008, MNRAS, 385, 1989
Huxor, A. P., Tanvir, N. R., Irwin, M. J., Ibata, R., Collett, J. L., Ferguson, A. M. N., Bridges, T., & Lewis, G. F. 2005, MNRAS, 360, 1007
Ibata, R., Martin, N. F., Irwin, M., Chapman, S., Ferguson, A. M. N., Lewis, G. F., & McConnachie, A. W. 2007, ApJ, 671, 1591
Ibata, R. A., Gilmore, G., & Irwin, M. J. 1994, Nature, 370, 194
Irwin, M., & Hatzidimitriou, D. 1995, MNRAS, 277, 1354
Irwin, M., & Lewis, J. 2001, NewA Rev., 45, 105
Irwin, M. J. 1994, in Dwarf Galaxies, ed. G. Meylan & P. Prugniel (Garching: ESO), 27
Irwin, M. J., Ferguson, A. M. N., Huxor, A. P., Tanvir, N. R., Ibata, R. A., & Lewis, G. F. 2008, ApJ, 676, L17
Irwin, M. J., et al. 2007, ApJ, 656, L13
Kalirai, J. S., et al. 2006, ApJ, 648, 389
Karachentsev, I. D., & Karachentseva, V. E. 1999, A&A, 341, 355
Klypin, A., Kravtsov, A. V., Valenzuela, O., & Prada, F. 1999, ApJ, 522, 82
Koch, A., & Grebel, E. K. 2006, AJ, 131, 1405
Kopylov, A. I., Tikhonov, N. A., Fabrika, S., Drozdovsky, I., & Valeev, A. F. 2008, MNRAS, 387, L45
Kravtsov, A. V., Gnedin, O. Y., & Klypin, A. A. 2004, ApJ, 609, 482
Krismer, M., Tully, R. B., & Gioia, I. M. 1995, AJ, 110, 1584
Kroupa, P., Theis, C., & Boily, C. M. 2005, A&A, 431, 517
Lee, M. G., Freedman, W. L., & Madore, B. F. 1993, ApJ, 417, 553
Lynden-Bell, D. 1976, MNRAS, 174, 695
———. 1982, Observatory, 102, 202
Majewski, S. R., Skrutskie, M. F., Weinberg, M. D., & Ostheimer, J. C. 2003, ApJ, 599, 1082
Majewski, S. R., et al. 2007, ApJ, 670, L9
Martin, N. F., de Jong, J., & Rix, H.-W. 2008, ApJ, 684, 1075
Martin, N. F., Ibata, R. A., & Irwin, M. 2007, ApJ, 668, L123
Martin, N. F., Ibata, R. A., Irwin, M. J., Chapman, S., Lewis, G. F., Ferguson, A. M. N., Tanvir, N., & McConnachie, A. W. 2006, MNRAS, 371, 1983
Mateo, M. L. 1998, ARA&A, 36, 435
Mayer, L., Mastropietro, C., Wadsley, J., Stadel, J., & Moore, B. 2006, MNRAS, 369, 1021
McConnachie, A. W., Arimoto, N., & Irwin, M. 2007a, MNRAS, 379, 379
McConnachie, A. W., & Irwin, M. J. 2006a, MNRAS, 365, 1263
———. 2006b, MNRAS, 365, 902

McConnachie, A. W., Irwin, M. J., Ferguson, A. M. N., Ibata, R. A., Lewis, G. F., & Tanvir, N. 2004, MNRAS, 350, 243
———. 2005, MNRAS, 356, 979
McConnachie, A. W., Venn, K. A., Irwin, M. J., Young, L. M., & Geehan, J. J. 2007b, ApJ, 671, L33
Merrett, H. R., et al. 2006, MNRAS, 369, 120
Metz, M., Kroupa, P., & Jerjen, H. 2007, MNRAS, 374, 1125
Moore, B., Quinn, T., Governato, F., Stadel, J., & Lake, G. 1999, MNRAS, 310, 1147
Morrison, H. L., Harding, P., Hurley-Keller, D., & Jacoby, G. 2003, ApJ, 596, L183
Peñarrubia, J., McConnachie, A. W., & Navarro, J. F. 2008a, ApJ, 672, 904
Peñarrubia, J., Navarro, J. F., & McConnachie, A. W. 2008b, ApJ, 673, 226
Sakai, S., Madore, B. F., & Freedman, W. L. 1999, ApJ, 511, 671
Sakamoto, T., & Hasegawa, T. 2006, ApJ, 653, L29
Salaris, M., & Cassisi, S. 1997, MNRAS, 289, 406
Sales, L. V., Navarro, J. F., Abadi, M. G., & Steinmetz, M. 2007, MNRAS, 379, 1475
Schlegel, D. J., Finkbeiner, D. P., & Davis, M. 1998, ApJ, 500, 525
Sharina, M. E., Karachentsev, I. D., & Tikhonov, N. A. 1997, Astron. Lett., 23, 373
Skillman, E. D. 2005, NewA Rev., 49, 453
Smecker-Hane, T. A., Stetson, P. B., Hesser, J. E., & Lehnert, M. D. 1994, AJ, 108, 507
Strigari, L. E., Bullock, J. S., Kaplinghat, M., Diemand, J., Kuhlen, M., & Madau, P. 2007a, ApJ, 669, 676
Strigari, L. E., Koushiappas, S. M., Bullock, J. S., & Kaplinghat, M. 2007b, Phys. Rev. D, 75, 083526
VandenBerg, D. A., Bergbusch, P. A., & Dowler, P. D. 2006, ApJS, 162, 375
VandenBerg, D. A., & Clem, J. L. 2003, AJ, 126, 778
Walsh, S. M., Jerjen, H., & Willman, B. 2007, ApJ, 662, L83
Whiting, A. B., Hau, G. K. T., & Irwin, M. 1999, AJ, 118, 2767
Whiting, A. B., Irwin, M. J., & Hau, G. K. T. 1997, AJ, 114, 996
Willman, B., Governato, F., Dalcanton, J. J., Reed, D., & Quinn, T. 2004, MNRAS, 353, 639
Willman, B., et al. 2005, ApJ, 626, L85
———. 2006, preprint (astro-ph/0603486)
Zucker, D. B., et al. 2004, ApJ, 612, L121
———. 2006a, ApJ, 643, L103
———. 2006b, ApJ, 650, L41
———. 2007, ApJ, 659, L21